SURFACE ROUGHNESS MODELING AND OPTIMIZATION IN ULTRASONIC VIBRATION-ASSISTED EDM OF HARDOX 500 USING RSM AND GPR APPROACHES

Nguyen Cong Danh[1,a*], Nguyen Manh Cuong[2,b], Mai Tat Loi[3,c], Tran Huu Danh[4,d]

[1]**Vinh Long Vocational College**, Phu Quoi Commune, Vinh Long Province, Vietnam
[2]**Thai Nguyen University of Technology**, Thai Nguyen University, Tich Luong Ward, Thai Nguyen, Vietnam
[3]**Vinh University of Technology Education**, Truong Vinh Ward, Nghe An Province, Vietnam
[4]**Vinh Long University of Technology Education**, Long Chau Ward, Vinh Long Province, Vietnam
[a]congdanh1104@gmail.com, [b]nmcuong@tnut.edu.vn, [c]maitatloi@vuted.edu.vn, [d]danhth@vlute.edu.vn
*Corresponding author

Received: 25/12/2025; Reviewed: 27/2/2026; Accepted: 04/5/2026

ABSTRACT

This study investigates the surface roughness behavior in ultrasonic vibration-assisted electrical discharge machining (UV-EDM) of Hardox 500 steel, a material known for its high hardness and wear resistance. A Box–Behnken experimental design was employed with five input parameters: vibration amplitude (A), pulse-on time (Ton), pulse-off time (Toff), discharge current (IP), and servo voltage (SV). The experimental data were first modeled using a response surface methodology (RSM) quadratic regression, which provided acceptable predictive capability (R^2 = 0.867). To enhance prediction accuracy, Gaussian process regression (GPR) models with different kernel–basis function combinations were evaluated. Among them, the Matern 3/2 kernel with a pure quadratic basis achieved the best performance (R^2 = 0.994, Adjusted R^2 = 0.993), significantly outperforming RSM. Optimization using the best GPR model identified the optimal process conditions (A = 3.22 µm, Ton = 8 µs, Toff = 12.20 µs, IP = 7.10 A, SV = 5.02 V), yielding a predicted minimum surface roughness of 2.56 µm. The findings demonstrate that GPR provides superior modeling accuracy over RSM, offering a reliable tool for surface quality improvement in UV-EDM of difficult-to-machine steels.

Keywords: *Ultrasonic vibration-assisted EDM; Hardox 500; Surface roughness; Response surface methodology (RSM); Gaussian process regression (GPR); Process optimization.*

1. INTRODUCTION

Electrical Discharge Machining (EDM) is a machining process widely used for shaping difficult-to-machine materials. However, conventional EDM is often limited by a low material removal rate, poor surface quality, and unstable debris removal. To overcome these limitations, Ultrasonic Vibration-Assisted Electrical Discharge Machining (UV-EDM) has emerged as a promising solution. The application of ultrasonic vibration enhances dielectric fluid circulation, improves debris removal efficiency, and stabilizes the plasma channel, thereby increasing machining performance and improving surface quality. Recent studies on UV-EDM have attracted increasing attention, demonstrating its significant potential for advanced manufacturing applications.

Numerous studies have highlighted the role of ultrasonic vibration in improving debris removal and stabilizing the electrical discharge process. Lei et al. [1] demonstrated that a composite electrode in UV-EDM enables efficient machining of enclosed micro-grooves with improved geometric accuracy. Han et al. [2] applied powder-mixed dielectric UV-EDM to TiN ceramics and reported significant improvements in both the material removal rate and surface morphology. Similarly, Wang et al. [3] showed that longitudinal/torsional ultrasonic vibration reduces taper and enhances debris removal during deep-hole EDM. These findings indicate that ultrasonic vibration assistance is a key factor in overcoming the inherent limitations of EDM when machining hard and brittle materials.

In addition to debris removal, ultrasonic vibration also affects the distribution of discharge energy. Choubey et al. [4] employed a finite element model to compare micro-EDM with and without ultrasonic vibration assistance, confirming higher energy efficiency and process stability under ultrasonic vibration. Hou and Bai [5] introduced a novel three-dimensional vibration mode to enhance debris removal efficiency, while Zhang et al. [6] further investigated the mechanism of debris motion in UV-EDM drilling. Experimental results reported by Yin et al. [7] and Chenxue et al. [8] demonstrated that longitudinal–torsional vibration and bubble dynamics under ultrasonic excitation significantly influence the discharge channel, thereby contributing to improved surface quality.

Another research direction focuses on the influence of electrode vibration modes on machining accuracy and surface integrity. Li et al. [9,10] investigated the application of a circular ultrasonic vibrating electrode in micro-EDM and demonstrated that this technique significantly reduces surface defects and improves hole quality. Hirao et al. [11] and Lin et al. [12] also reported that applying ultrasonic vibration to either the electrode or the dielectric fluid promotes a more uniform discharge distribution and enhances surface characteristics. Xing et al. [13] and Wang [14] investigated the effects of machining parameters and found that an optimal ultrasonic vibration frequency reduces surface roughness and improves the stability of the material removal process.

Although the aforementioned studies have highlighted the positive effects of ultrasonic vibration, most have primarily focused on qualitative improvements in machining performance, dimensional accuracy, or material removal mechanisms. Only a limited number of studies have systematically modeled and optimized surface roughness (Ra) in UV-EDM, particularly when machining hard or ultra-hard materials such as Hardox 500, which is well known for its excellent wear resistance and widespread industrial applications. Previous modeling approaches based on empirical regression or finite element simulation [4,14,15] have provided useful solutions; however, their prediction accuracy is often insufficient for precise optimization. Furthermore, recent studies have rarely employed advanced machine learning models such as Gaussian Process Regression (GPR), which has demonstrated strong potential for capturing nonlinear interactions and achieving superior prediction accuracy compared with the conventional Response Surface Methodology (RSM)**.**

Therefore, a significant research gap exists in developing accurate predictive models and robust optimization frameworks for surface roughness in UV-EDM of Hardox 500 steel. Addressing this research gap is essential to ensure surface integrity and to expand the applicability of EDM for machining difficult-to-machine alloys.

The objective of this study is to systematically model and optimize surface roughness in UV-EDM of Hardox 500 steel. A Box–Behnken Design (BBD) was employed to evaluate the effects of vibration amplitude, pulse-on time, pulse-off time, discharge current, and servo voltage. The experimental data were modeled using Response Surface Methodology (RSM) and subsequently compared with advanced Gaussian Process Regression (GPR) models incorporating different kernel–basis function combinations. The best-performing GPR model was then employed for optimization to determine the machining conditions that minimize surface roughness (Ra). The results confirm the superiority of GPR over RSM in predictive modeling and provide an optimal set of machining parameters for achieving high surface quality in UV-EDM of Hardox 500 steel.

2. CONTENT

2.1. Experimental Procedure

2.1.1. Experimental Equipment, Materials, and Procedure

Figure 1 illustrates the experimental setup used in this study. The UV-EDM experiments were conducted on a Sodick A30 CNC EDM machine, which enables precise control of the machining parameters. The ultrasonic vibration system consisted of an MPI WG-3000 ultrasonic generator (Switzerland) with a maximum power output of 3000 W, coupled with an RPS-5020-4Z transducer (2000 W, operating frequency of 20 kHz). In this study, a horn designed to operate at a frequency of 20 kHz [16] was employed to transmit ultrasonic vibration to the workpiece.

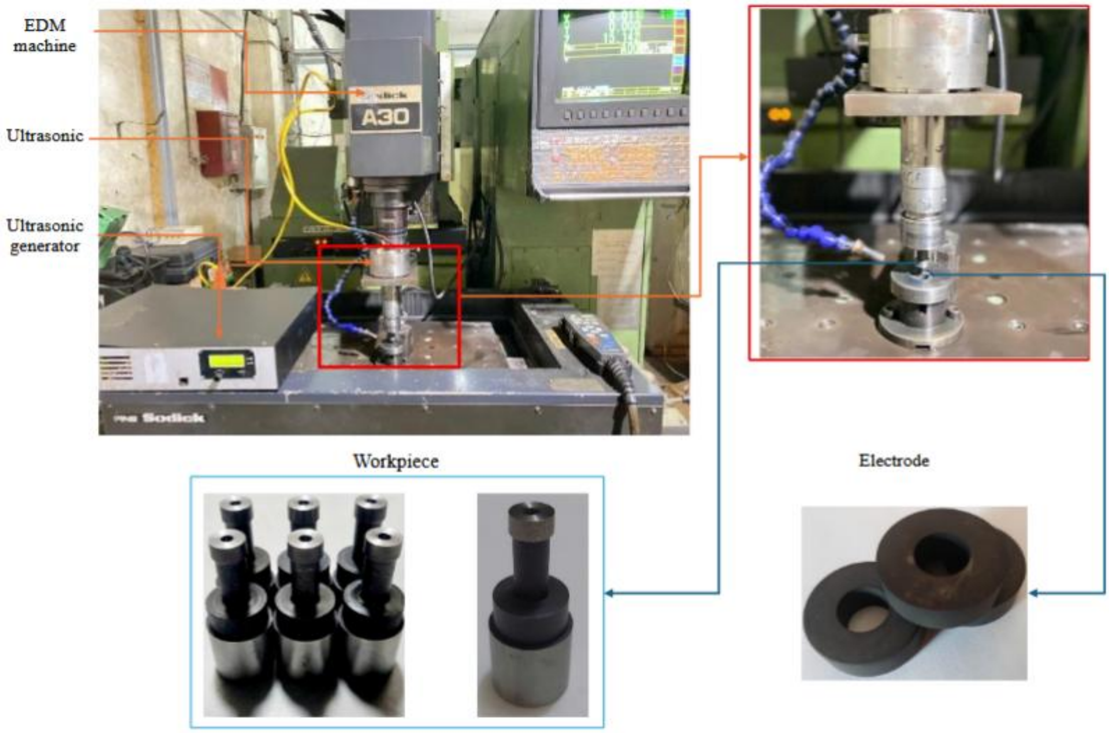

Figure 1. *Experimental setup*

The electrode material used in all experiments was HK2 graphite, which possesses high electrical conductivity, low thermal deformation, and reasonable cost. The workpiece material was HARDOX 500 steel, which is characterized by high hardness and excellent wear resistance and is widely used in the mining industry and heavy-duty equipment. Diel MS 7000 dielectric oil (Total, France) was used as the dielectric fluid.

To investigate the effects of machining parameters on surface roughness (Ra) in UV-EDM, the experiments were designed using the Box–Behnken Design (BBD). This method enables the simultaneous evaluation of multiple factors with a reasonable number of experimental runs, thereby ensuring the efficiency and reliability of the collected data.

In this study, the five input machining parameters were ultrasonic vibration amplitude A (μm), pulse-on time Ton (μs), pulse-off time Toff (μs), discharge current Ip (A), and servo voltage SV (V).

2.1.2. Measurement and Data Processing Methods

The output response was surface roughness Ra (μm), which was measured using a Mitutoyo SV3100 surface roughness tester (Japan) supplied by FUTU1 Company (Song Cong, Thai

Nguyen). Surface roughness was measured at three different locations along the machined cylindrical surface, and the average value was taken as the representative result.

A total of 46 experiments were conducted according to the BBD matrix, ensuring a balanced distribution of parameter combinations. The experimental design and the measured Ra values are presented in Table 1.

Table 1. *Experimental design and measured surface roughness results*

No.	A (µm)	Ton (µs)	Toff (µs)	IP (A)	SV (V)	Ra (µm)
1	1.2	8	12	10	5	3.353
2	1.2	16	12	10	5	6.569
3	5.2	8	12	10	5	3.198
4	5.2	16	12	10	5	5.711
5	3.2	12	8	5	5	7.220
6	3.2	12	8	15	5	6.764
7	3.2	12	16	5	5	6.462
8	3.2	12	16	15	5	7.260
9	3.2	8	12	10	4	3.175
10	3.2	8	12	10	6	3.201
11	3.2	16	12	10	4	5.889
12	3.2	16	12	10	6	6.588
13	1.2	12	8	10	5	5.418
14	1.2	12	16	10	5	4.492
15	5.2	12	8	10	5	5.444
16	5.2	12	16	10	5	4.959
17	3.2	12	12	5	4	6.339
18	3.2	12	12	5	6	5.968
19	3.2	12	12	15	4	6.726
20	3.2	12	12	15	6	7.312
21	3.2	8	8	10	5	3.430
22	3.2	8	16	10	5	3.256
23	3.2	16	8	10	5	7.280
24	3.2	16	16	10	5	5.313
25	1.2	12	12	5	5	6.730
26	1.2	12	12	15	5	7.595
27	5.2	12	12	5	5	6.099
28	5.2	12	12	15	5	8.799
29	3.2	12	8	10	4	5.790
30	3.2	12	8	10	6	5.019
31	3.2	12	16	10	4	5.287
32	3.2	12	16	10	6	5.479
33	1.2	12	12	10	4	4.408
34	1.2	12	12	10	6	5.259
35	5.2	12	12	10	4	6.312
36	5.2	12	12	10	6	5.564
37	3.2	8	12	5	5	2.965
38	3.2	8	12	15	5	3.850
39	3.2	16	12	5	5	7.694
40	3.2	16	12	15	5	12.089

41	3.2	12	12	10	5	4.483
42	3.2	12	12	10	5	4.919
43	3.2	12	12	10	5	5.483
44	3.2	12	12	10	5	5.032
45	3.2	12	12	10	5	5.455
46	3.2	12	12	10	5	4.785

2.2. Results and Discussion

2.2.1. Effects of Machining Parameters on Surface Roughness (Ra)

The experimental results and regression analysis indicate that surface roughness (Ra) is simultaneously affected by multiple machining parameters with different levels of influence. To clarify the role of each factor, analysis of variance (ANOVA), main effects plots, and effect bar charts were employed. Figure 2 illustrates the effects of the machining parameters on Ra.

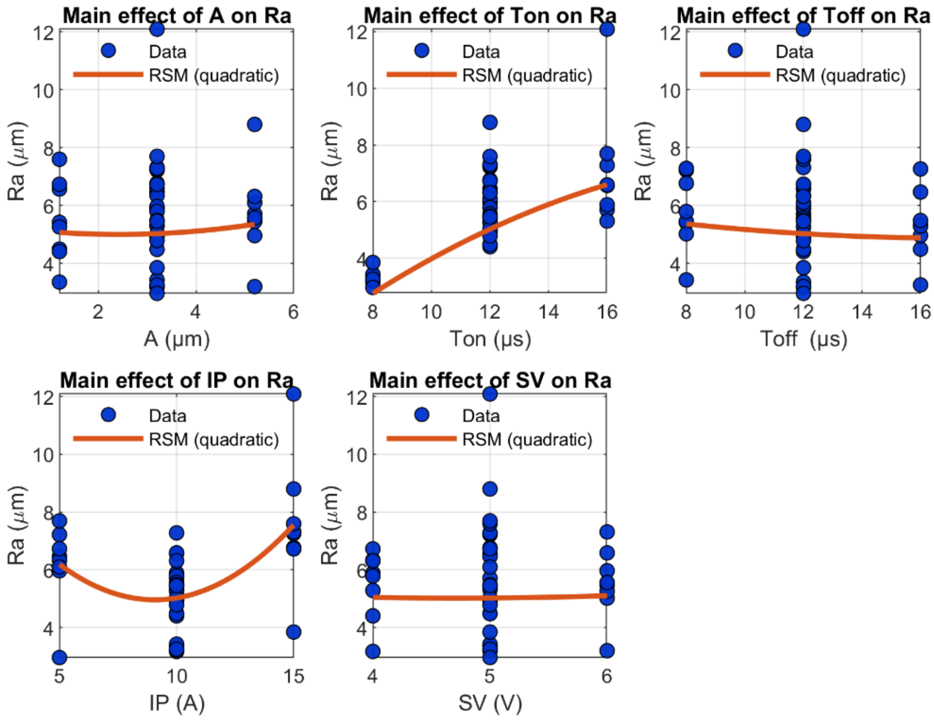

Figure 2. *Effects of machining parameters on Ra*

Effect of discharge current (Ip):

Discharge current is the most influential factor affecting Ra. The quadratic regression curve indicates a nonlinear relationship: as Ip increases from a low level (~5–7 A) to a medium level (~8–9 A), Ra decreases slightly due to a more stable discharge arc and more uniform material removal. However, when Ip exceeds 10 A, Ra increases significantly because the higher discharge energy causes excessive melting and the formation of deeper craters, resulting in a rougher surface. The ANOVA results confirm that both Ip and its quadratic term are statistically significant ($p < 0.01$).

Effect of pulse-on time (Ton):

Ra increases noticeably with increasing pulse-on time. A longer pulse-on time accumulates more discharge energy during each pulse, resulting in the formation of larger and deeper craters, thereby increasing surface roughness. The ANOVA results indicate that both Ton and its interaction with Ip are statistically significant.

Effect of pulse-off time (Toff):

The effect of Toff on Ra is relatively small but shows a slight decreasing trend, with higher Toff values generally resulting in lower Ra. This is because a longer pulse-off time allows the dielectric fluid to recover and improves debris removal. However, the influence of Toff remains weak within the investigated range.

Effect of ultrasonic vibration amplitude (A):

The ultrasonic vibration amplitude (A) has a certain effect on Ra, but its influence is weaker than that of Ip and Ton. Increasing A from 1.2 µm to 5.2 µm results in only a slight variation in Ra. Ultrasonic vibration improves debris removal and reduces the occurrence of sustained arcing; however, its effect is less pronounced than that of the discharge energy parameters.

Effect of servo voltage (SV):

SV has no significant effect on Ra within the investigated range. The main effects plot of SV is nearly flat, and the ANOVA results ($p > 0.6$) confirm that this parameter has no statistically significant influence.

Table 2 presents the ANOVA results for Ra based on the quadratic regression model.

ANOVA results for Ra:

Table 2. *ANOVA results for Ra*

Term	DF (Degrees of freedom)	Sum of Squares (Sum Sq)	Mean Square (Mean Sq)	F-value	p-value	η_p^2 (partial)
Linear	5	67.6348	13.5270	19.6891	6.01×10^{-8}	0.7975
Nonlinear	15	44.1489	2.9433	4.2841	6.74×10^{-4}	0.7199
Residual	25	17.1757	0.6870	—	—	0.5000
Lack of fit	20	16.4182	0.8209	5.4186	3.49×10^{-2}	0.4887
Pure error	5	0.7575	0.1515	—	—	0.0422

General remarks:

Surface roughness (Ra) is strongly influenced by discharge current Ip (particularly the nonlinear term Ip^2) and pulse-on time Ton, whereas pulse-off time Toff and ultrasonic vibration amplitude A have relatively minor effects, and the influence of SV is negligible. Owing to the presence of lack-of-fit, the quadratic regression model does not fully capture the nonlinear characteristics of the Ra data. Therefore, Gaussian Process Regression (GPR) was employed in the subsequent analyses to improve prediction accuracy and optimize the machining conditions for minimizing Ra while maintaining a balance with the material removal rate (MRR).

2.2.2. Development of the Experimental Regression Model for Ra

a) Ra modeling using the RSM method

Quadratic regression analysis for Ra yielded a coefficient of determination of $R^2 = 0.8668$ and an adjusted coefficient of determination of $R^2 = 0.7603$, indicating that the model explains approximately 76–87% of the variation in the experimental data. The resulting quadratic regression equation is presented in Equation (1).

$$\begin{aligned} Ra = {} & 14.6701 + 0.4187A + 0.7575Ton - 0.3690Toff - 2.4409IP - 1.5302SV \\ & - 0.0219A \cdot Ton + 0.0138A \cdot Toff + 0.0459A \cdot IP - 0.2000A \cdot SV \\ & - 0.0280Ton \cdot Toff + 0.0439Ton \cdot IP + 0.0421Ton \cdot SV \\ & + 0.0157Toff \cdot IP + 0.0601Toff \cdot SV + 0.0479IP \cdot SV \\ & + 0.0456A^2 - 0.0217Ton^2 + 0.0060Toff^2 + 0.0738IP^2 + 0.0494SV^2 \end{aligned} \tag{1}$$

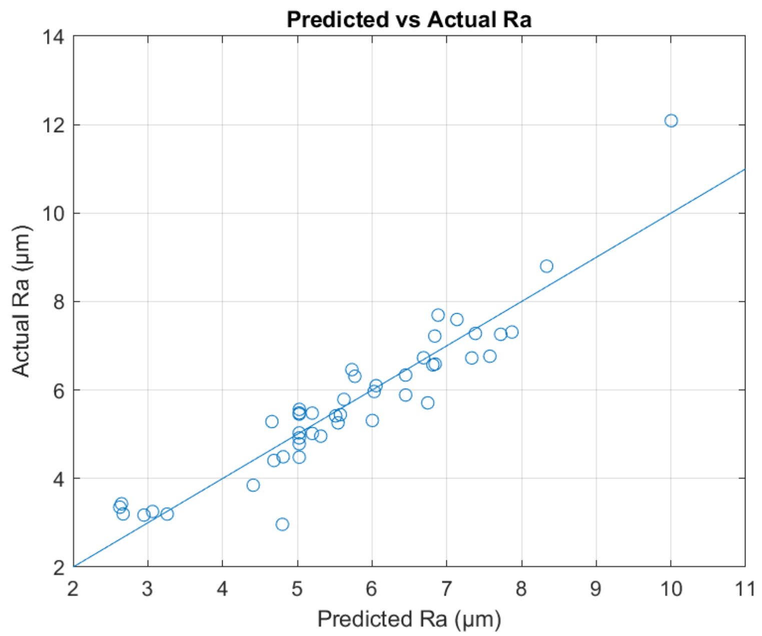

Figure 3. *Predicted versus experimental Ra values using the RSM model*

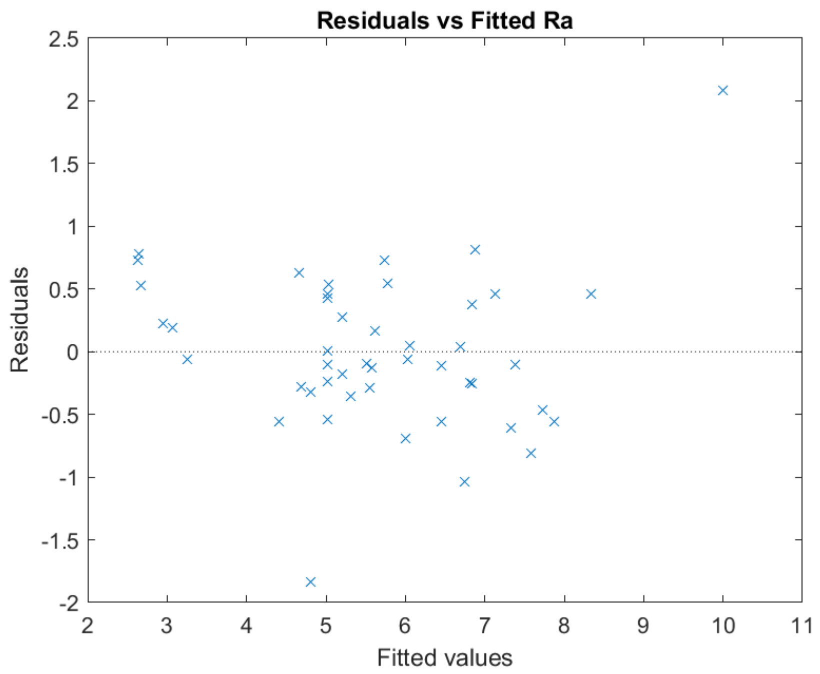

Figure 4. *Residuals versus predicted values for the RSM model*

To evaluate the goodness-of-fit of the model, Figure 3 illustrates the relationship between the predicted and experimental Ra values. The data points are distributed close to the diagonal line, indicating good agreement between the model predictions and the experimental results. Figure 4 presents the residuals versus predicted values, where the residuals are randomly scattered around the centerline, suggesting that the RSM model exhibits no systematic bias and provides an acceptable fit.

(b) Improving prediction using Gaussian Process Regression (GPR)

To improve prediction accuracy, multiple combinations of Gaussian Process Regression (GPR) kernel and basis functions were compared. Their performance, evaluated using R^2 and adjusted R^2 (R^2_adj), is summarized in Table 3.

Table 3. Comparison of kernel–basis configurations of GPR for Ra

Kernel	Basis	R^2	R^2_{adj}
Squaredexponential	Constant	0.9529	0.9470
Squaredexponential	Linear	0.9560	0.9506
Squaredexponential	Purequadratic	0.8164	0.7934
Rational quadratic	Constant	0.9590	0.9539
Rational quadratic	Linear	0.9556	0.9501
Rational quadratic	Purequadratic	0.9941	0.9934
Matern32	Constant	0.9771	0.9743
Matern32	Linear	0.9906	0.9894
Matern32	Purequadratic	0.9941	0.9934
Matern52	Constant	0.9814	0.9791
Matern52	Linear	0.9615	0.9567
Matern52	Purequadratic	0.9922	0.9912

The results show that the rationalquadratic + pureQuadratic and matern32 + pureQuadratic models achieved the highest prediction accuracy, with an R^2 of 0.9941 and an adjusted R^2 of 0.9934. In this study, the matern32 + pureQuadratic model was selected because of its better generalization capability.

Optimization using this model in MATLAB identified the optimal machining parameters for minimizing Ra as follows: A = 3.2230 µm, Ton = 8.0000 µs, Toff = 12.1999 µs, Ip = 7.0955 A, and SV = 5.0160 V. The predicted minimum Ra was 2.5649 µm.

Figure 5 illustrates the performance of the best GPR model (matern32 + pureQuadratic). Compared with the RSM model, the data points are distributed closer to the diagonal line, indicating higher prediction accuracy and superior model robustness.

Figure 5 illustrates the performance of the best GPR model (matern32 + pureQuadratic). Compared with the RSM model, the data points are distributed closer to the diagonal line, indicating higher prediction accuracy and superior model robustness.

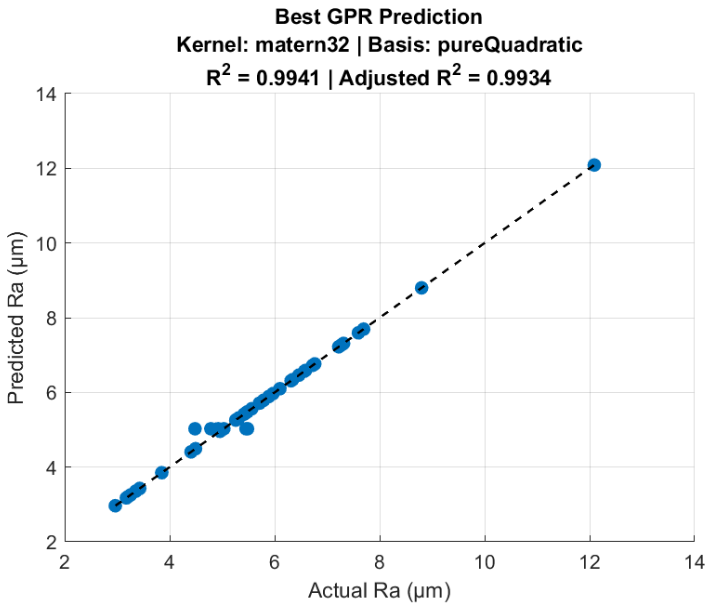

Figure 5. *Predicted vs. experimental Ra values using the GPR (matern32–pureQuadratic) model.*

3. CONCLUSION

The present study investigated the surface roughness characteristics in ultrasonic vibration-assisted electrical discharge machining (UV-EDM) of HARDOX 500 steel using a graphite electrode. A comprehensive experimental design and comparative modeling approach were employed to evaluate the effects of machining parameters and to develop an accurate predictive model. Based on the experimental and simulation results, the following conclusions can be drawn:

1. Experimental results: Surface roughness (Ra) in UV-EDM is strongly influenced by discharge current (Ip) and pulse-on time (Ton), whereas pulse-off time (Toff) and ultrasonic vibration amplitude (A) have moderate effects, while servo voltage (SV) exhibits a negligible influence within the investigated range. ANOVA confirms the high statistical significance of Ip and Ton, particularly the nonlinear term Ip^2.

2. RSM analysis: The quadratic regression model developed using the Response Surface Methodology (RSM) achieved acceptable prediction accuracy, with an R^2 of 0.8668 and an adjusted R^2 of 0.7603. Although the model captures the overall trend of the experimental data, the presence of lack-of-fit indicates that RSM has limitations in describing the nonlinear behavior of Ra.

3. GPR analysis: The Gaussian Process Regression (GPR) model demonstrated superior performance compared with the RSM model. Among the investigated kernel–basis configurations, the matern32–pureQuadratic model achieved the highest prediction accuracy, with an R^2 of 0.9941 and an adjusted R^2 of 0.9934, demonstrating its excellent capability to capture complex nonlinear relationships while providing stable and reliable predictions.

4. Optimization results: Using the optimal GPR model, the optimum machining parameters for minimizing Ra were determined as: A = 3.223 µm, Ton = 8.0 µs, Toff = 12.20 µs, Ip = 7.10 A, and SV = 5.02 V. Under these conditions, the minimum predicted Ra was 2.56 µm, demonstrating the effectiveness of the proposed model in guiding process optimization.

5. Overall contribution: This study demonstrates that, while RSM provides a reasonable baseline approach, GPR is a more powerful and accurate tool for modeling and optimizing surface roughness in UV-EDM of difficult-to-machine materials such as HARDOX 500 steel. These findings contribute to the advancement of predictive modeling frameworks and provide practical guidance for improving surface quality in hybrid EDM processes.

Acknowledgements

The authors would like to express their sincere gratitude to the Ministry of Education and Training of Vietnam (MOET) for supporting this research through Project B2024-TNA-18. The authors also sincerely acknowledge Thai Ha Precision Mechanical Private Enterprise and the University of Technology, Thai Nguyen University for providing laboratory facilities and technical support throughout this study.

References

[1] J. Lei, H. Shen, H. Wu, W. Pan, X. Wu, and C. Zhao, "Ultrasonic vibration-assisted electrical discharge machining of enclosed microgrooves with laminated electrodes," *Journal of Materials Research and Technology,* vol. 30, pp. 9521-9530, 2024.

[2] J. Han, X. Gao, Y. Zhou, Z. Li, M. Gao, and Q. Zhang, "Machining characteristics in ultrasonic vibration-assisted powder-mixed electrical discharge machining of TiN ceramics," *Ceramics International,* vol. 50, no. 8, pp. 13478-13489, 2024.

[3] P. Wang *et al.*, "Debris motion and taper suppression in EDM deep hole machining assisted by longitudinal/torsional ultrasonic vibration," *Journal of Manufacturing Processes,* vol. 133, pp. 798-810, 2025.

[4] M. Choubey, K. Maity, and A. Sharma, "Finite element modeling of material removal rate in micro-EDM process with and without ultrasonic vibration," *Grey Systems: Theory and Application,* vol. 10, no. 3, pp. 311-319, 2020.

[5] S. Hou and J. Bai, "A novel ultrasonic vibration-assisted micro-EDM method to improve debris removal performance using relative three-dimensional ultrasonic vibration (RTDUV)," The International Journal of Advanced Manufacturing Technology, vol. 127, no. 11-12, pp. 5711-5727, 2023.

[6] P. Zhang *et al.*, "Investigating mechanisms of debris removal in ultrasonic vibration-assisted EDM drilling," *International Journal of Mechanical Sciences,* vol. 279, p. 109486, 2024.

[7] Z. Yin *et al.*, "A novel EDM method using longitudinal-torsional ultrasonic vibration (LTV) electrodes to improve machining performance for micro-holes," *Journal of Manufacturing Processes,* vol. 102, pp. 231-243, 2023.

[8] W. Chenxue, T. Sasaki, and A. Hirao, "Observation of bubble behavior in EDM with ultrasonic vibration," *Procedia CIRP,* vol. 113, pp. 267-272, 2022.

[9] Z. Li, J. Tang, Y. Li, and J. Bai, "Investigation on surface integrity in novel micro-EDM with two-dimensional ultrasonic circular vibration (UCV) electrode. J Manuf Process 76: 828–840," ed, 2022.

[10] Z. Li, J. Tang, and J. Bai, "A novel micro-EDM method to improve microhole machining performances using ultrasonic circular vibration (UCV) electrode," *International Journal of Mechanical Sciences,* vol. 175, p. 105574, 2020

[11] A. Hirao, H. Gotoh, and T. Tani, "Some effects on EDM characteristics by assisted ultrasonic vibration of the tool electrode," *Procedia Cirp,* vol. 68, pp. 76-80, 2018.

[12] Y.-C. Lin, J.-C. Hung, H.-M. Chow, A.-C. Wang, and J.-T. Chen, "Machining characteristics of a hybrid process of EDM in gas combined with ultrasonic vibration and AJM," *Procedia CIRP,* vol. 42, pp. 167-172, 2016.

[13] Q. Xing, Z. Yao, and Q. Zhang, "Effects of processing parameters on processing performances of ultrasonic vibration-assisted micro-EDM," *The International Journal of Advanced Manufacturing Technology,* vol. 112, pp. 71-86, 2021.

[14] Y. Wang *et al.*, "Analysis of material removal and surface generation mechanism of ultrasonic vibration–assisted EDM," *The International Journal of Advanced Manufacturing Technology,* vol. 110, pp. 177-189, 2020.

[15] M. R. Shabgard, A. Gholipoor, and M. Mohammadpourfard, "Numerical and experimental study of the effects of ultrasonic vibrations of tool on machining characteristics of EDM process," *The International Journal of Advanced Manufacturing Technology,* vol. 96, pp. 2657-2669, 2018.

[16] V.-T. Dinh, T.-Q. Le, D.-B. Vu, N.-P. Vu, and T.-L. Mai, "Ultrasonic EDM for External Cylindrical Surface Machining with Graphite Electrodes: Horn Design and Hybrid NSGA-II–AHP Optimization of MRR and Ra," *Machines,* vol. 13, no. 8, p. 675, 2025.